

Phase transitions in $\text{Pb}[(\text{Ni}_{1/3}\text{Sb}_{2/3})_x\text{Ti}_y\text{Zr}_z]\text{O}_3$ solid solution ceramics studied by piezoelectric measurements

Irena Jankowska-Sumara

Received: 7 August 2009 / Accepted: 21 April 2010 / Published online: 2 May 2010
© Springer Science+Business Media, LLC 2010

Abstract The piezoelectric properties of $\text{Pb}[(\text{Ni}_{1/3}\text{Sb}_{2/3})_x\text{Ti}_y\text{Zr}_z]\text{O}_3$ solid solution, where $x+y+z=1$, $x=0.08$ and $y=0.44\text{--}0.49$ have been investigated in a wide temperature region using a resonance technique. The physical properties of PZT near the morphotropic phase boundary modified with the relaxor $\text{Pb}(\text{Ni}_{1/3}\text{Sb}_{2/3})\text{O}_3$ have been studied. The coefficients s_{11} , k_{31} and d_{31} have been calculated basing on the damped harmonic oscillator model of piezoelectrically vibrating sample. Several anomalies in the temperature dependence of piezoelectric coefficients within the temperature range from 300 to 600 K have been found. For $y>0.46$ the coexistence of rhombohedral and tetragonal phases occurs. The observed low piezoelectric activity confirms the existence of polar regions above T_m in $\text{Pb}[(\text{Ni}_{1/3}\text{Sb}_{2/3})_x\text{Ti}_y\text{Zr}_z]\text{O}_3$.

Keywords PNS-PZT ceramics · Piezoelectric effect · Phase transitions

1 Introduction

It is obvious that the aim of investigations of ferroelectric materials is the possibility to use these materials in wide range of applications. They possess very good piezoelectric, pyroelectric and dielectric properties and their use as actuators and sensors is well known [1–11]. On the other hand elastic constants calculated from piezoelectric experiments allow describing the low-frequency crystal lattice dynamics near the structural phase transition.

Piezoelectric ceramics based on $\text{PbZr}_{1-x}\text{Ti}_x\text{O}_3$ perovskites (PZT) show excellent piezoelectric properties especially near so called Morphotropic Phase Boundary (MPB), a boundary between the rhombohedral and tetragonal phases [2]. High strains near the MPB in this compound seem to result from a coupling between two equivalent energy states i.e. the tetragonal (P4mm) and rhombohedral (R3m) phases [12, 13]. Noheda *et al* have discovered a monoclinic phase near the MPB what have thrown a new light on the phase diagram in PZT and on the origin of strong piezoelectricity. The discovery of this phase provides an explanation for the high piezoelectric response [14–17], although this problem has not been resolved yet.

Recently it has been found that solid PZT solutions with complex perovskite relaxors such as PMN, PZN, PNN and PFS [18–26] exhibit excellent both electromechanical and pyroelectric properties.

$\text{Pb}[(\text{Ni}_{1/3}\text{Sb}_{2/3})_x\text{Ti}_y\text{Zr}_z]\text{O}_3$ where $x+y+z=1$, $x=0.08$ and $y=0.44\text{--}0.49$ is an interesting solid solution obtained basing on PZT. It was described for the first time by Helke and Röder from the structural and piezoelectric properties point of view [27–29]. According to the phase diagram obtained from structural investigations the MPB exists in this material near the composition of $y=0.46$. Similar conclusion was obtained from the pyroelectric measurements [30]. However there are no new works about this promising system in literature. Hence, it is important to study the piezoelectric activity of $\text{Pb}[(\text{Ni}_{1/3}\text{Sb}_{2/3})_x\text{Ti}_y\text{Zr}_z]\text{O}_3$ solid solution in details, especially by passage the phase transition points. The observation of the piezo-effect was carried out using a well known dynamic method based on piezoelectric resonance detection. This technique allows the simultaneous determination of the complex elastic coefficients, piezoelectric tensor and electromechanical coupling factor.

I. Jankowska-Sumara (✉)
Institute of Physics, Pedagogical University,
ul. Podchorążych 2,
Kraków 30-084, Poland
e-mail: ijsumara@ap.krakow.pl

2 Experimental conditions

The measurements were performed on $\text{Pb}[(\text{Ni}_{1/3}\text{Sb}_{2/3})_x\text{Ti}_y\text{Zr}_z]\text{O}_3$ ceramics (abbreviated to PNS-PZ-yPT) where $x+y+z=1$, $x=0.08$ and $y=0.44\text{--}0.49$. The density of ceramics was determined by the Archimedes method. The mean density of the samples was about 7500 kg/m^3 . The samples with the shape of thin bars with dimensions $3*1*0.5 \text{ mm}^3$ were polished and the largest surfaces were covered with silver electrodes. The electric contact was made by means of thin silver wires glued in the centre of electrodes. The dielectric characterization of the samples was made with an HP 4263 LCR meter at frequencies 100 Hz, 1 kHz, 10 kHz, and 100 kHz. The temperature was controlled to within $\pm 0.1 \text{ K}$ using a programmable temperature controller. The dielectric measurements were made in the temperature range 300–650 K. For piezoelectric measurements the specimens were poled in a d.c. electric field. The most effective poling was obtained under the field of 5 kV/cm. The poling processes were made from 600 K down to room temperature maintaining the field strength. From the geometrical configuration adapted in the experiment, the d_{31} , k_{31} —piezoelectric and s_{11} —elastic coefficients could have been measured [2].

By using a circuit presented in [2] the absolute admittance $|Y|$ frequency spectrum was obtained and used to determine the transverse piezoelectric strain constants. Total admittance of any dielectric material and thus also of a vibrating bar may be represented by a complex quantity $Y=G+iB$ consisting of conductance G (real part) and susceptance B (imaginary part) [31].

One can show that:

$$\frac{B}{\omega} = \frac{\beta}{M} \frac{\omega_o^2 - \omega^2}{(\omega_o^2 - \omega^2)^2 + \omega^2 \Gamma^2} + C' \quad (1)$$

$$\frac{G}{\omega} = \frac{\beta}{M} \frac{\omega \Gamma}{(\omega_o^2 - \omega^2)^2 + \omega^2 \Gamma^2} + C''_o \quad (2)$$

where M is mass of the bar, ω_o ($2\pi f_o$)—free running frequency, Γ ($2\pi\gamma$)—damping coefficient and β is a constant, C'_o and C''_o are respectively the real and imaginary part of the sample capacity at frequencies outside the piezoelectric resonance. These relations are the main functions to which the absolute admittance can be fitted:

$$|Y| = \sqrt{B^2 + G^2} \quad (3)$$

By fitting the experimental data to the Eq. 3 and having ω_o and Γ it is possible to calculate the real s' and imaginary s'' part of the complex elastic coefficient. The complex elastic coefficient fulfils the following relation [31, 32]:

$$s_{11} = s'_{11} - i s''_{11} = \frac{1}{4f_o^2 l^2 \rho} - i \frac{1}{4f_o^2 l^2 \rho} \left(\frac{\gamma}{f_o} \right) \quad (4)$$

where ρ is the density of sample, l is the length of bar and f_o is the resonance frequency.

The piezoelectric coupling coefficient k_{31} can be got from the resonance (f_o) and antiresonance (f_a) frequencies [2, 33]:

$$\frac{k_{31}^2}{1 - k_{31}^2} = \frac{\pi}{2} \frac{f_a}{f_o} \tan \left(\frac{\pi}{2} \frac{\Delta f}{f_o} \right) \quad (5)$$

The piezoelectric coefficient d_{31} can be calculated from the following expression:

$$d_{31} = k_{31} \sqrt{\varepsilon_{33} s_{11}^E} \quad (6)$$

3 Experimental result

3.1 Dielectric properties

The compositional dependence of dielectric response and corresponding loss tangent characteristics for PNS-PZ-yPT ceramics are shown in Fig. 1 for the compositions with y from 0.44 to 0.49. The increase in y gradually shifts T_m and ε'_{max} appears at higher temperatures, although the maximum of ε' is shifted by about 60 K down to lower temperatures in comparison with pure PZT composition. The dielectric peak of ε' and $\tan \delta$ were also found to be broadened which can be attributed to substantial fluctuations and a structural disorder usually linked to the presence of ferroelectric relaxor. Nevertheless the temperature dependence of dielectric permittivity does not resemble that one found for classical relaxor, in particular the broad maxima of ε' and $\tan \delta$ are not frequency dependent (Fig. 2). For this reason the observed dispersion can not be caused by the relaxational dynamics of polar nanoclusters. The most probable mechanism responsible for the observed dielectric dispersion can be related to the electronic conductivity.

3.2 Piezoelectric properties

The temperature evolutions of piezoelectric signals are presented in Fig. 3(a-f). The figures show typical piezoelectric characteristics with resonance and antiresonance frequencies. Local small signals below and above the main resonance signals follows probably from the incomplete polarization process in the sample. With increasing temperature the piezoelectric signal changes its strength and frequency position. Even above T_m very weak signals were recorded.

Table 1 Dielectric and piezoelectric properties of PNS-PZ-yPT ceramics at room temperature

PNS-PZ-yPT	T_m (K)	Piezoelectric properties at room temperature				
		d_{31} (C/N)	k_{31}	s'_{11} (m^2/N)	s''_{11} (m^2/N)	Q_m
$y=0.44$	540	$92 \cdot 10^{-12}$	0.23	$6 \cdot 10^{-12}$	$0.1 \cdot 10^{-12}$	60
$y=0.45$	541	$100 \cdot 10^{-12}$	0.32	$12 \cdot 10^{-12}$	$0.17 \cdot 10^{-12}$	70.5
$y=0.46$	544	$121 \cdot 10^{-12}$	0.34	$14.2 \cdot 10^{-12}$	$0.18 \cdot 10^{-12}$	78
$y=0.47$	545	$127 \cdot 10^{-12}$	0.36	$16.8 \cdot 10^{-12}$	$0.19 \cdot 10^{-12}$	84
$y=0.48$	552	$110 \cdot 10^{-12}$	0.32	$12.3 \cdot 10^{-12}$	$0.2 \cdot 10^{-12}$	61.5
$y=0.49$	554	$90 \cdot 10^{-12}$	0.28	$11.5 \cdot 10^{-12}$	$0.25 \cdot 10^{-12}$	46

An example of the fit to the Eq. 3 is shown in Fig. 4. Using the Eqs. 4–6 the values of piezoelectric coefficients and real and imaginary parts of elastic constants were calculated. The calculated form fits the values of the piezoelectric and elastic coefficients at room temperature are collected in Table 1 in function of composition.

The thermal behaviour of these coefficients for two chosen ceramics of concentration below ($y=0.45$) and above ($y=0.48$) of the value for MPB is presented in Figs. 5

and 6. Two different behaviours for these samples can be observed. In the case of PNS-PZ-0.45PT sample the characteristics show clear anomalies (Fig. 5). The d_{31} and s'_{11} coefficients show a broad maximum near T_m corresponding to the phase transition point. The similar behaviour was previously observed in the measurements of the pyroelectric effect [30]. First, the coefficient k_{31} is constant (up to about 440 K) and than continuously lowers down. Close to 440 K the imaginary part of elastic coefficient s''_{11} also possesses a broad maximum. The distinct increase of the imaginary part of s''_{11} can be accounted for the increasing damping of acoustic wave in this temperature range. According to the phase diagram [28], the symmetry of the PNS-PZ-0.45PT at room temperature is rhombohedral.

With increasing temperature, it transforms into the tetragonal symmetry. It has been established that in PZT from MPB region the rhombohedral and tetragonal phases coexist [34]. This coexistence is equivalent to the structural disorder with a complicated domain and domain walls structure. Thus, this disorder may be responsible for the distinct damping of the piezoelectric vibrations.

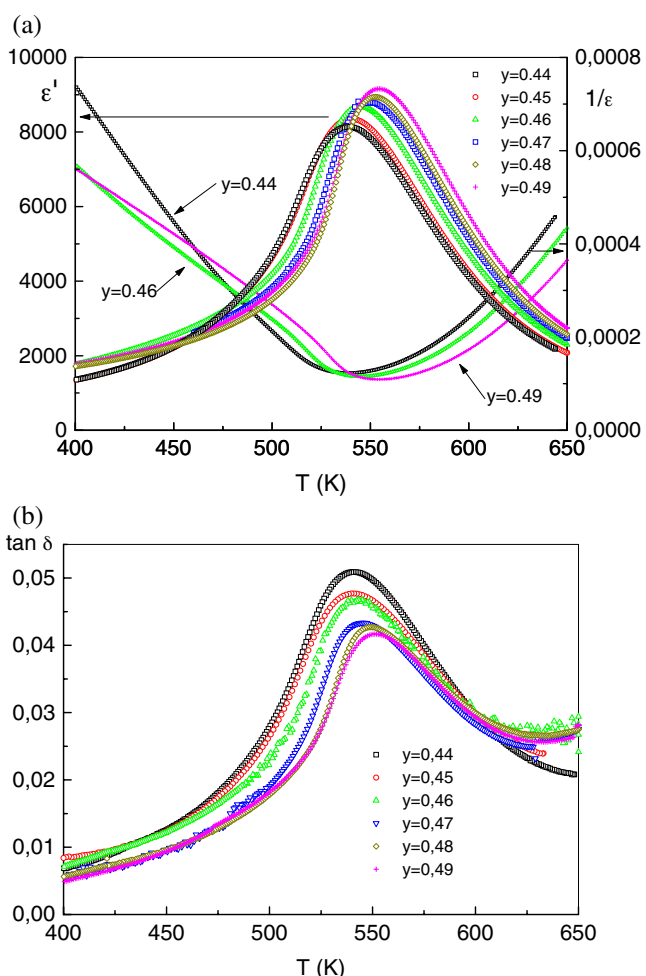


Fig. 1 Variations of ϵ' , $1/\epsilon'$ (a) and $\tan \delta$ (b) with temperature for PNS-PZ-yPT samples

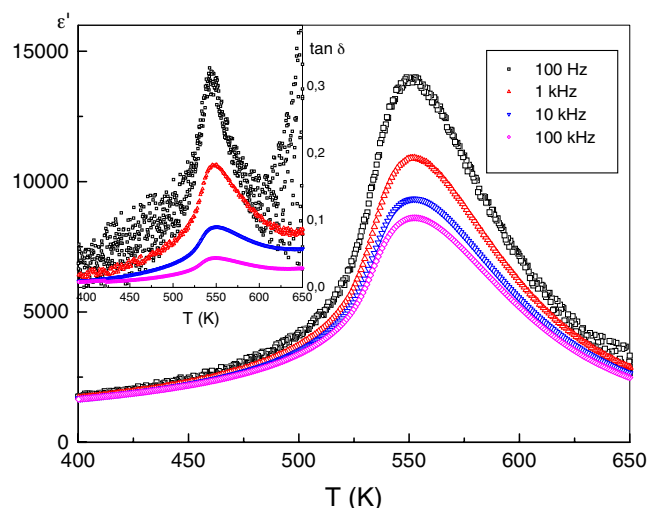


Fig. 2 Variation of ϵ' and $\tan \delta$ (in the inset) with frequency and temperature for PNS-PZ-0.48PT sample

Fig. 3 Temperature evolutions of longitudinal frequency responses of poled ceramic bars of $\text{Pb}[(\text{Fe}_{1/3}\text{Sb}_{2/3})_{0.1}\text{Ti}_y\text{Zr}_{0.9-y}]_3$ with different concentrations of y

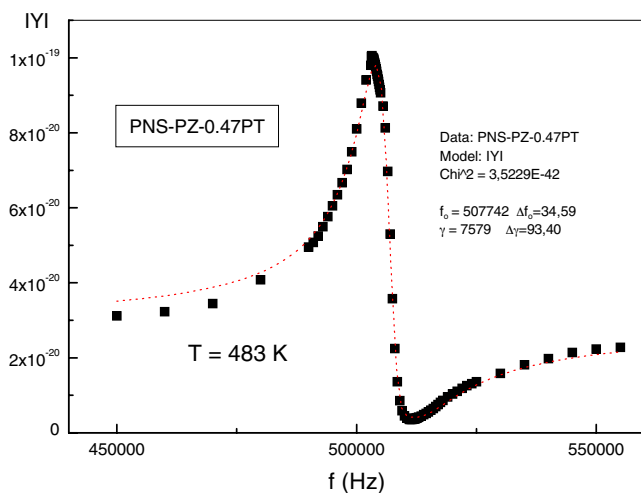
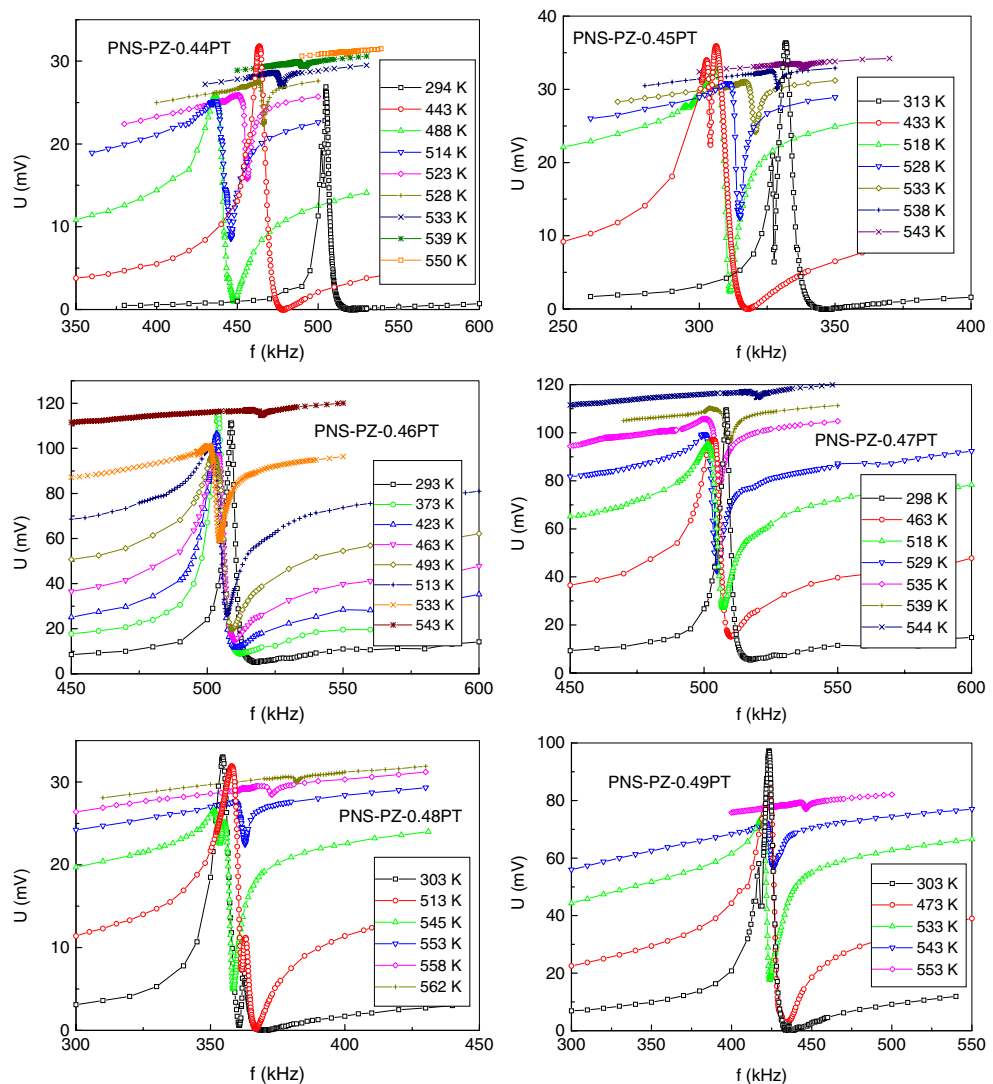


Fig. 4 The sample fit of the experimental data to the function (3) (the absolute admittance is expressed here in arbitrary units)

Above the range of MPB temperature dependences of the piezoelectric coefficients are quite different (Fig. 6). All characteristics show sharp anomalies at 550 K. At the same temperature a single sharp peak in the pyroelectric measurements was also observed [30]. The anomalies were found which correspond directly to the phase transition from the tetragonal to cubic phase. In the inset of Fig. 6a the temperature dependence of $1/s'_{11}$ is presented. It is worth noting that in the temperature range below T_m this dependence resembles the soft mode behaviour. This softening comes from the coupling of the acoustic phonon with the soft phonon optic mode in the tetragonal phase [35].

Above 550 K the piezoelectric coefficients rapidly decrease but do not disappear. The stable piezoelectric signal can be observed even several degrees above T_m . The source of piezoelectric activity is, in our opinion, connected with the polar clusters existence. Until their size and

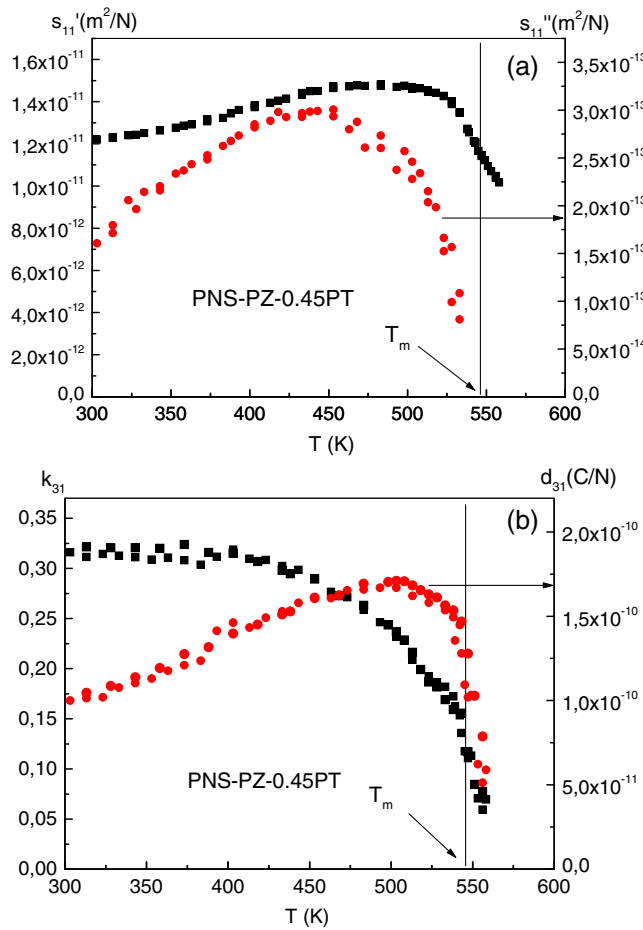


Fig. 5 Temperature runs for the elastic modulus s'_{11} and s''_{11} (a) and piezoelectric coefficients d_{31} and k_{31} (b) for $\text{Pb}[(\text{Ni}_{1/3}\text{Sb}_{2/3})_{0.08}\text{Ti}_{0.45}\text{Zr}_{0.47}]\text{O}_3$ ceramic

correlation radius are large enough the interaction between polar clusters through the non-polar matrix influences the macroscopic piezoelectric response.

4 Conclusions

The influence of relaxor $\text{Pb}(\text{Ni}_{1/3}\text{Sb}_{2/3})\text{O}_3$ on piezoelectric properties of PZT ceramics from the range of morphotropic phase boundary has been studied. This kind of modification provides the following features. In comparison with pure PZT the maximum of ε' is shifted by about 60 K to lower temperatures. It was established that for the PNS-PZ- y PT solid solution the MPB exists for $y=0.46$. For all measured samples the piezoelectric activity reveals the weak temperature dependence in the low temperature range.

Below the value of y corresponding with MPB the changes of piezoelectric d_{31} and elastic s'_{11} , s''_{11} coefficients are continuous and show broad local maxima. The piezoelectric coupling factor k_{31} is constant up to 440 K and than continuously decreases. It is known that the

imaginary part of material constant is usually more sensitive to the abnormal behaviour of physical properties than the real part. That is why the temperature dependence of the imaginary part of elastic coefficient is represented by a broad maximum near 440 K. The coexistence of the rhombohedral and tetragonal phases in this temperature region reflects the structural disorder that influences the damping of acoustic modes.

For compositions with value of y near to that for the MPB the piezoelectric coefficients show sharp anomalies at temperatures corresponding to transition to the cubic phase. This indicates that in these samples the tetragonal phase plays dominant role below T_m . Moreover the temperature dependence of $1/s'_{11}$ resembles the soft mode behaviour of the acoustic phonon near the phase transition point. This is an evidence that in PNS-PZ- y PT with $y>0.46$ the polarization is coupled with the elastic properties.

Above T_m the piezoelectric signal although very small, is still observed. The presence of the pyroelectric signals above T_m [30] points to the existence of polar regions. Thought the clear relaxor properties were not found in these

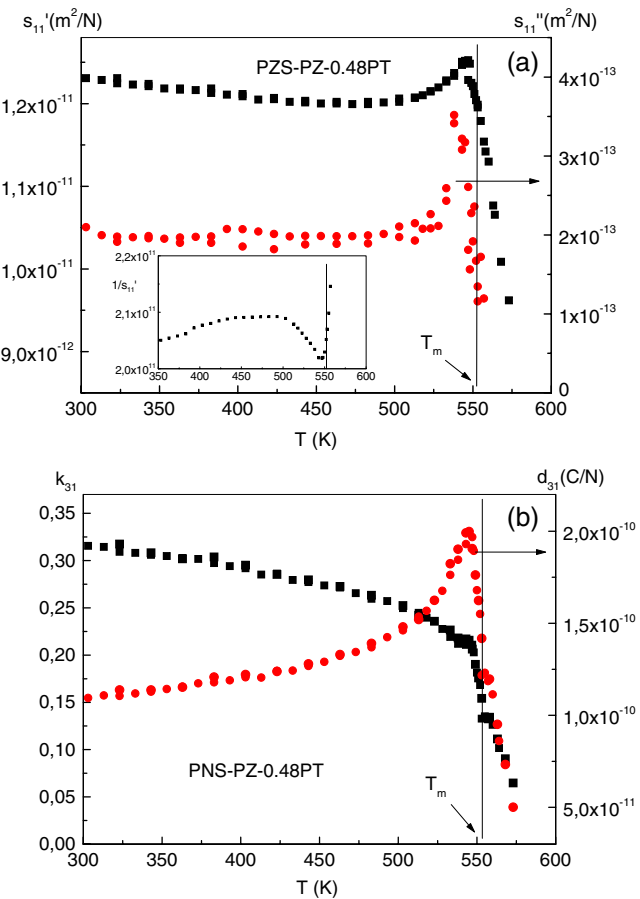


Fig. 6 Temperature runs for the elastic modulus s'_{11} and s''_{11} (a) and piezoelectric coefficients d_{31} and k_{31} (b) for $\text{Pb}[(\text{Ni}_{1/3}\text{Sb}_{2/3})_{0.08}\text{Ti}_{0.48}\text{Zr}_{0.44}]\text{O}_3$ ceramic

materials (see Fig. 2); the polar regions which are present above T_m can interact between themselves in non-trivial way and constitute a polar subsystem in the paraelectric matrix. These regions after ordering in d.c. electric field lead to the weak piezoelectric signal appearance. Such a subsystem has already been proved to exist even in normal ferroelectric—barium titanate on the basis of electrostrictive measurements [36]. Measurements of electrostrictive properties for the presented compositions will be additional evidence for the existence of the polar regions in paraelectric phase.

Acknowledgments This work was partially supported by the State Committee of Scientific research (KBN). The author is grateful to dr A. Osak from the Institute of Physics, Cracow University of Technology for supplying the ceramics.

References

1. H. Jaffe, D.A. Berlincourt, Piezoelectric Transduces materials. Proc. IEEE **53**, 1372–86 (1965)
2. B. Jaffe, R.W. Cook, H. Jaffe, *Piezoelectric Ceramics* (Academic, London, 1971)
3. J.M. Herbert, *(Ferroelectric transducers and sensors)* (Gordon and Breach, New York, 1982)
4. R.W. Whatmore, P.C. Osbond, N.M. Shorocks, Ferroelectrics **76**, 1 (1987)
5. Y. Xu, *Ferroelectric Materials and Their Applications*, North Holland, Amsterdam, (1991)
6. K. Uchino, *(Piezoelectric actuators and ultrasonic motors)* (Kluwer, Boston, 1997)
7. M.B. Lines, A.M. Glass, *(Principles and applications of ferroelectrics and related materials)* (Clarendon, Oxford, 1997)
8. G.M. Haerling, J. Am. Ceram. Soc. **82**, 797–8181 (1999)
9. C.P. Shaw, S. Gupta, S.B. Stringfellow, A. Nawarro, J.R. Alcock, R.W. Whatmore, J. Eur. Cer. Soc **22**, 2123 (2002)
10. R.W. Whatmore, O. Molter, C.P. Shaw, J. Eur. Ceram. Soc **23**, 721 (2003)
11. S. B. Lang, Phys. Today 31, (2005)
12. W. Cao, L.E. Cross, Phys. Rev. B **47**, 4825 (1993)
13. G.A. Rossetti Jr., W. Zhang, A.G. Khachaturyan, Appl. Phys. Lett. **88**, 072912 (2006)
14. C.A. Guarany, L.H.Z. Pelaio, K. Yukimitu, J.C.S. Morales, J.A. Eiras, J. Phys.: Condens. Matter **15**, 4851 (2003)
15. B. Noheda, J.A. Gonzalo, L.E. Cross, R. Guo, S.E. Park, D.E. Cox, G. Shirane Phys. Rev. B **61**, 8687 (2000)
16. B. Noheda, D.E. Cox, G. Shirane, R. Guo, B. Jones, L.E. Cross, Phys. Rev. B **63**, 014103 (2000)
17. R. Guo, L.E. Cross, S.E. Park, B. Noheda, D.E. Cox, G. Shirane, Phys. Rev. Lett. **84**, 5423 (2000)
18. X. Zhu, Z. Meng, J Mater Sci **31**, 2171 (1996)
19. T. Takenaka, A.S. Bahalla, L.E. Cross, K. Sakata, J. Am. Ceram. Soc. **72**, 1016 (1989)
20. V. Shilnikov, A.V. Sopit, A.I. Burhanov, A.G. Luchaninov, J. Eur. Ceram. Soc **19**, 1295 (1999)
21. V. Kowal, C. Alemany, J. Brancin, H. Brunckowa, J. Electroceram. **10**, 19 (2003)
22. Z.G. Zhu, B.S. Li, G.R. Li, W.Z. Zhang, Q.R. Yin Mat, Sci. Eng. B **117**, 216 (2005)
23. H. Du, Qu , J. Che, Z. Pei and W. Zhou, J. Electroceram. **21**, 589 (2008)
24. A.P. Osak, M. Pawełczyk, W.S. Ptak, Ferroelectrics **186**, 123 (1996)
25. I. Jankowska-Sumara, Ferroelectrics **345**, 115 (2006)
26. I. Jankowska-Sumara, A. Osak, Phase Transitions **81**, 331 (2008)
27. G. Helke, Hermsdorfer Techn. Mitt. **2**, 1010 (1971)
28. G. Helke, W. Kirsch, Hermsdorfer Techn. Mitt. **44**, 1456 (1977)
29. G. Helke, G. Röder, Hermsdorfer Techn. Mitt. **54**, 1729 (1979)
30. I. Jankowska-Sumara, A. Osak, Physica B **404**, 3698 (2009)
31. A.M. Gonzalez, C. Alemany, J. Phys. D: Appl. Phys. **29**, 247 (1996)
32. D.A. Berlicourt, D.R. Curran, H. Jaffe, Physical Acoustic Principles and Methods **1**, 169 (1964)
33. IEEE Standard on Piezoelectricity, ANSI/IEEE Std. 176 (1987)
34. B. Noheda, J. A .Gonzalo, A. Caballero, C. Moure, D. E. Cox, G. Shirane, arXiv,cond-mat/9907286v1 (1999)
35. J. Petzelt, Y.G. Goncharov, G.V. Kozlov, A.A. Volkov, B. Wyncke, F. Brehat, Czech J. Phys B **34**, 887 (1984)
36. K. Wieczorek, A. Ziębińska, Z. Ujma, K. Szot, M. Górný, I. Franke, J. Koperski, A. Soszyński, K. Roleder, Electrostrictive and Piezoelectric Effect in BaTiO₃ and PbZrO₃. Ferroelectrics **336**, 61 (2006)